Paracoccus pantotrophus Pseudoazurin Is an Electron Donor to Cytochrome *c* Peroxidase†

Sofia R. Pauleta,‡,§ Françoise Guerlesquin,|| Celia F. Goodhew,§ Bart Devreese,⊥ Jozef Van Beeumen,⊥ Alice S. Pereira,‡ Isabel Moura,‡ and Graham W. Pettigrew*,§

ReQuimte, Centro de Química Física e Biotecnologia, FCT/UNL, Quinta da Torre, 2829-516 Caparica, Portugal, Royal (Dick) School of Veterinary Studies, The University of Edinburgh, Summerhall, Edinburgh, EH9 1QH, Scotland, U.K., Unité de Bioénergétique et Ingénierie des Protéines, IBSM-CNRS, 31 Chemin Joseph Aiguier, 13402, Marseille Cedex 20, France, and Laboratory of Protein Biochemistry, State University of Gent, B-9000 Gent, Belgium

Received May 1, 2004; Revised Manuscript Received June 21, 2004

ABSTRACT: The gene for pseudoazurin was isolated from *Paracoccus pantotrophus* LMD 52.44 and expressed in a heterologous system with a yield of 54.3 mg of pure protein per liter of culture. The gene and protein were shown to be identical to those from *P. pantotrophus* LMD 82.5. The extinction coefficient of the protein was re-evaluated and was found to be 3.00 mM^{-1} cm^{-1} at 590 nm. It was confirmed that the oxidized protein is in a weak monomer/dimer equilibrium that is ionic-strength-dependent. The pseudoazurin was shown to be a highly active electron donor to cytochrome *c* peroxidase, and activity showed an ionic strength dependence consistent with an electrostatic interaction. The pseudoazurin has a very large dipole moment, the vector of which is positioned at the putative electron-transfer site, His81, and is conserved in this position across a wide range of blue copper proteins. Binding of the peroxidase to pseudoazurin causes perturbation of a set of NMR resonances associated with residues on the His81 face, including a ring of lysine residues. These lysines are associated with acidic residues just back from the rim, the resonances of which are also affected by binding to the peroxidase. We propose that these acidic residues moderate the electrostatic influence of the lysines and so ensure that specific charge interactions do not form across the interface with the peroxidase.

c-type cytochromes and blue copper proteins are structurally very different, but Williams et al. (*1*) proposed that they share features of an electron-transfer surface that confers "pseudospecificity" in their interactions with a range of redox partners. There are two facets to this: one redox enzyme may bind more than one small redox protein as alternatives at a single reactive site; also, one small redox protein may be required to bind to more than one redox enzyme using the same reactive surface.

There are several instances of a type-I copper protein and a cytochrome acting as alternative "pseudospecific" carriers, depending on metal availability. *Pseudomonas aeruginosa* azurin can replace cytochrome c_{551} (*2*), and cyanobacterial plastocyanin and cytochrome c_6 are both competent in the transport of electrons from the cytochrome *bf* complex to photosystem I (*3*). In higher organisms, this flexibility has disappeared, with higher plant chloroplasts having only plastocyanin and mitochondria having only cytochrome *c*.

In previous studies (*4*, *5*), we have characterized the binding and kinetics of the nonphysiological electron donor (horse cytochrome *c*) and the physiological electron donor (cytochrome c_{550}), with cytochrome *c* peroxidase from *Paracoccus pantotrophus* LMD 52.44. Although, by analogy with other systems, pseudoazurin was suspected to be a second physiological electron donor, we have been unable to identify pseudoazurin in extracts of *P. pantotrophus* LMD 52.44, although it has been isolated and extensively characterized from the closely related strain LMD 82.5 and also from *P. denitrificans* LMD 22.21.

In *P. pantotrophus* LMD 82.5, the gene is under the control of the transcriptional activator FnrP (*6*), which regulates the expression of proteins (including pseudoazurin) that are required under anaerobic conditions (*7*, *8*). Pseudoazurin is proposed to be one of the electron carriers in the periplasm of the bacteria, shuttling electrons between the cytochrome bc_1 complex and several periplasmic enzymes involved in denitrification [cytochrome cd_1 nitrite reductase (*6*, *9*, *10*), nitric oxide reductase, and nitrous oxide reductase (*11*, *12*)]. However, it is not alone in that role; another small redox protein, the cytochrome c_{550}, has also been identified as the electron donor to these enzymes (*10*, *11*). Some preliminary studies have indicated that pseudoazurin can be a substrate for cytochrome *c* peroxidase in *P. pantotrophus* LMD 82.5 (*13*). In this paper, we show that the gene for the pseudoazurin is present in *P. pantotrophus* LMD 52.44 and

† This work was support with a Ph.D. grant from Fundação para a Ciência e Tecnologia (BD/18297/98) to S.R.P. G.W.P. thanks the BBSRC for financial support (Grant B13005). J.V.B. is indebted to the FWO-Flanders for Grant 0282.01.

* To whom correspondence should be addressed. E-mail: g.pettigrew@ed.ac.uk.

‡ Centro de Química Física e Biotecnologia.

§ The University of Edinburgh.

|| Unité de Bioénergétique et Ingénierie des Protéines.

⊥ State University of Gent.

10.1021/bi0491144 CCC: $27.50
Published on Web 08/11/2004

is identical to that of *P. pantotrophus* LMD 82.5. The recombinant protein can be expressed in *Escherichia coli* and is competent as an alternative electron donor to *P. pantotrophus* cytochrome *c* peroxidase.

In the case of cytochrome c_{550} and pseudoazurin, Williams et al. (*1*) proposed that the pseudospecific surface is composed of a hydrophobic patch that surrounds the exposed haem edge or the exposed histidine ligand, around which there is a ring of positively charged lysines. The work of Koppenol et al. (*14*) has shown that a useful way of considering charge asymmetry of a protein is the orientation and the magnitude of the dipole moment. For example, mitochondrial cytochrome *c* has a large dipole moment orientated toward the proposed electron-transfer site at the exposed haem edge. Koppenol and Margoliash (*15*) show that this dipole moment is instrumental in the preorientation of the cytochrome against the negatively charged surface of its redox partners, a process that leads to rate enhancement. We have shown that cytochrome c_{550} has a dipole moment more than 3 times the magnitude of that of horse cytochrome *c* but again positioned at the exposed haem edge (*16*). Here, we evaluate the dipole moment of pseudoazurin and its relatives.

The role of electrostatics and hydrophobic effects in the formation and stability of transient electron-transfer complexes has been carefully analyzed for the case of cytochrome *f* and plastocyanin (a structural relative of the pseudoazurin studied here) (*17*, *18*). We discuss our results in the light of these studies and propose a model in which the dipole moment plays an important role in preorientation, while charge compensation of lysines ensures that the binding affinity is not so great as to compromise dissociation or to lead to the formation of unproductive complexes.

MATERIALS AND METHODS

Strains, Vectors, and Growth Conditions. P. pantotrophus LMD 82.5 [previously named *Thiosphaera pantotropha* LMD 82.5 (*19*)] was grown under low aeration at 33 °C, in a nitrate liquid medium (*20*). In the final stage of growth, the trace metals solution of Kuenen et al. (*21*) was omitted. *P. pantotrophus* LMD 52.44 [previously named *P. denitrificans* LMD 52.44 (*19*)] was grown as previously described (*22*). Both types of culture were harvested and stored as described in ref *22*.

E. coli XL1-BLUE (Stratagene) was used for subcloning and grown aerobically in Luria−Bertani (LB) medium (*23*), supplemented with 100 μg/mL ampicillin, at 37 °C. *E. coli* BL21(DE3) (Stratagene) was used for expression of *P. pantotrophus* LMD 52.44 pseudoazurin and grown aerobically at 37 °C in LB medium supplemented with 100 μg/mL ampicillin and 0.5 mM $CuSO_4$, for 24 h, without induction. Orbital shaking was reduced in speed to avoid foaming. To label pseudoazurin with ^{15}N, the same clone was grown in a modified version of M9 medium (*23*) containing 1.0 g/L $^{15}NH_4Cl$ (*Isotec*), 3.0 g/L KH_2PO_4, 6.0 g/L $Na_2HPO_4{\cdot}7H_2O$, 0.5 g/L NaCl, 1.2% glucose, 1 mM $MgSO_4$, 0.01 mg/mL thiamine-HCl, 0.01 mM $CuSO_4$, 18.5 μM $FeCl_3{\cdot}6H_2O$, 0.1 mM $CaCl_2{\cdot}2H_2O$, and 100 μg/mL ampicillin. Addition of IPTG[1] was not used as a procedure because it did not improve the total pseudoazurin yield and damaged the outer membrane of the bacteria.

Construction of Recombinant Plasmid for Expression of P. pantotrophus LMD 52.44 Pseudoazurin. The pseudoazurin gene, including the signal peptide, was amplified by PCR using DNA from isolated colonies of *P. pantotrophus* LMD 52.44 as a template. The primers were designed according to the previously published sequence of the pseudoazurin gene from *P. pantotrophus* LMD 82.5 (*24*), forward primer = 5′-CCATGAATTCGTCGACAAGAAGGAGATATACATACATGTTCCACCATTCCC-3′ and reverse primer = 5′-TTACTGCAGGATCCCGGTCAGTTGACCTGGGC-3′.

The amplified DNA fragment (500 bp) was cloned into pGEM-T Easy vector (Promega), in the multiple-cloning site, and cut at *Eco*R I and *Spe* I sequences located in the *lac*Z gene. The resulting vector, pGEM-psaz, was then isolated and digested with the restriction enzymes *Bam*H I/*Afl* III (Gibco BRL). The DNA fragment containing the pseudoazurin gene including its signal sequence, was cloned into the *Nco* I/*Bam*H I restricted pET 21-d vector (Novagen) (treated with alkaline phosphatase after restriction to avoid recircularisation), yielding pET-psaz. The sequence of the isolated gene was found to be identical to that published for *P. pantotrophus* LMD 82.5 (*24*). All other molecular biology techniques were performed according to Sambrook et al. (*23*).

Purification of Pseudoazurin. Pseudoazurin isolated from *P. pantotrophus* LMD 82.5 was purified in a three-step procedure different from the one previously reported (*9*) and without precipitation with ammonium sulfate. Spheroplasts from *P. pantotrophus* LMD 82.5 were produced by lysozyme/EDTA treatment (*22*, *25*). The periplasmic fraction was loaded onto an anion-exchange chromatography DEAE-cellulose column (9 × 3 cm Ø). The column was eluted with a linear gradient in 10 mM Tris-HCl at pH 8.0 and 4 °C and 0−400 mM NaCl. The fractions containing pseudoazurin (identified by their blue color and higher absorbance at 590 nm) were pooled, diluted 5 times in cold distilled water, and concentrated on a small DEAE-cellulose column (1.5 × 1 cm Ø). The protein was eluted with 10 mM Tris-HCl, 500 mM NaCl at pH 8.0 and 4 °C. Three preparations of pseudoazurin were combined and loaded onto a Sephadex G75-50 column (80 × 3 cm Ø), equilibrated with 20 mM Tris-HCl at pH 8.0 and 4 °C and 100 mM NaCl. The fractions containing pseudoazurin were combined and concentrated as before. The buffer was exchanged to 20 mM Tris-HCl at pH 7.3 and 20 °C, using a Vivaspin membrane with M_r cut off of 5000, prior to loading onto a Phenomenex BIOSEP-DEAE-p anion-exchange column. The protein was eluted at 0.5 mL/min with a linear gradient of 100 min between 20 mM Tris-HCl at pH 7.3 and 20 °C and 20 mM Tris-HCl at pH 7.3 and 20 °C and 400 mM NaCl. The fractions containing pure pseudoazurin ($A_{590nm}/A_{278nm} \geq 0.6$) were concentrated above a Vivaspin membrane, and the buffer was changed to 10 mM Mes and 10 mM NaCl at pH 6.0. The protein was stored at −40 °C.

For the heterologously expressed pseudoazurin from *P. pantotrophus* LMD 52.44, recombinant *E. coli* cells were

[1] Abbreviations: Mes, 2-[*N*-morpholino]ethane-sulfonic acid; Hepes, *N*-[2-hydroxyethyl]piperazine-*N*′-[2-ethanesulfonic acid]; DAD, 2,3,5,6-tetramethyl-*p*-phenylene-diamine; IPTG, isopropyl β-D-thiogalactopyranoside; SDS, sodium dodecyl sulfate; TNBS, trinitrobenzene sulfonate; FnrP, fumarate and nitrate reductase regulatory protein; Ø, diameter.

harvested by centrifugation at 4500*g* for 25 min, at 4° C. The cell pellet (approximately 4 g/L) was resuspended in 8 mL/g cells and 100 mM Tris-HCl at pH 7.3. The release of pseudoazurin was achieved by 5 freeze−thaw cycles followed by centrifugation at 15000*g*, for 30 min, at 4° C. The pseudoazurin was recovered in the reduced state and was oxidized by addition of potassium ferricyanide. Subsequent purification followed the same procedure as before for *P. pantotrophus* LMD 82.5 (see above) but omitted the last step of BIOSEP-DEAE-P chromatography, which proved unnecessary. Typically, 4.0 μmol (54.3 mg) of pseudoazurin was obtained from 1 L of LB medium.

Both the purified pseudoazurin from *P. pantotrophus* LMD 82.5 and the heterologously expressed pseudozurin from *P. pantotrophus* LMD 52.44 had a ratio of $A_{590nm}/A_{278nm} \geq 0.6$ when completely oxidized. These preparations were considered to be pure as judged by silver staining of SDS and native PAGE and by the BIOSEP-DEAE-P chromatographic pattern (data not shown).

Purification of Other Proteins. Cytochrome c_{550} and cytochrome *c* peroxidase from *P. pantotrophus* LMD 52.44 were purified as previously described (*22*).

Determination of the Extinction Coefficient of Pseudoazurin: (i) Copper Determination. Two methods were used. In the first, the total amount of copper present in solution was estimated using an inductively coupled plasma (ICP) atomic emission spectrometer (Thermo Jarrell Ash IRIS). In the second, the Cu^I content was determined using a modified version of the method of Hanna et al. (*26*), which is based on the formation of a complex between Cu^I and 2, 2′-biquinoline in an acetic acid medium. All solutions were prepared fresh in deionized water. A sample of pseudoazurin (100 μL, containing 10−30 nmol of protein) or a standard solution of copper acetate was reduced by adding 300 μL of 20 mM sodium ascorbate (in 0.1 M sodium phosphate at pH 6.0) and incubated for 10 min. To this, 600 μL of a 2, 2′-biquinoline solution (0.5 mg/mL) prepared in glacial acetic acid was added, and the solution was incubated for 10 min prior to the measurement of the absorbance at 546 nm. The concentration of Cu^I present in each sample was determined using the slope of the calibration curve prepared with copper-(II) acetate. The extinction coefficient obtained (6.3 mM^{-1} cm^{-1}) was identical to that described by Hanna et al. (*26*).

(ii) Protein Determination: (a) Free Amino Groups. The estimation of free amino groups was performed using the TNBS method (*27*, *28*). Approximately 2.5−5 nmol of pseudoazurin (in 0.25 mL) were incubated with 0.25 mL of 0.1% TNBS (Sigma) prepared in deionized water and 0.25 mL of 4% $NaHCO_3$ at pH 8.5 and 40 °C for 2 h, protected from the light. Afterward, 0.25 mL of 10% SDS and 0.125 mL of 1 M HCl were added to stop the reaction and the concentration of free amino groups was determined using the extinction coefficient of 14 mM^{-1} cm^{-1} for the trinitrophenyl group (*29*). The protein concentration was obtained assuming the known amino acid composition of pseudoazurin, which contains 10 lysine residues and 1 free α amine.

(b) Lowry/Biuret Method. The method used was a modified version of the Lowry/Biuret method (*30*). To 0.1 mL of sample, 0.4 mL of Biuret reagent was added and incubated for 10 min at room temperature; after addition of 3.5 mL of 2.3% Na_2CO_3 and 0.1 mL of Folin-Ciocalteu's phenol reagent, the sample was incubated for 30 min at room temperature before the measurement of the absorbance at 750 nm. The standard protein used was bovine serum albumin.

(c) Bradford Method. Protein concentration was also estimated using the Bradford assay (*31*, *32*). The reagents were obtained as a BioRad kit, and assays were carried out according to the instructions of the manufacturer, with bovine serum albumin as a standard protein. The same standard solution was used for both the Lowry/Biuret and the Bradford methods.

(iii) UV-Visible Spectroscopy. The spectra of pseudoazurin were determined between 250 and 850 nm in 10 mM phosphate buffer at pH 7.0. Complete oxidation was obtained by addition of a crystal of potassium ferricyanide. The protein was reduced with sodium dithionite. Parallel determination of copper, protein, and UV-visible spectra was carried out using the same parent solution.

Enzymatic Activity of Cytochrome c Peroxidase with Different Electron Donors. The activity of mixed-valence cytochrome *c* peroxidase, in the presence of calcium ions, was measured by following the decrease in absorbance of the ferrocytochrome *c* α band at 550 nm (*4*) or the increase in absorbance of the pseudoazurin at 590 nm as oxidation occurred. The pseudoazurin and cytochromes *c* were reduced with 1 mM sodium ascorbate, and the reducing agent was removed using a Sephadex G25 column equilibrated in the assay buffer. For all experiments, the enzyme was activated for 30 min at 4 °C by dilution to 2 μM in the assay buffer containing 1 mM $CaCl_2$, 1 mM sodium ascorbate, and 5 μM DAD.

Assays were initiated by addition of the enzyme (1−2 nM) to a cuvette containing 10 mM Mes at pH 6.0, 1 mM $CaCl_2$, 20 μM horse ferrocytochrome *c*, ferrocytochrome c_{550}, or pseudoazurin, 36 μM hydrogen peroxide, and 0, 10, 25, 50, 100, 200, or 500 mM NaCl.

For the determination of K_m, the conditions in the cuvette were 5 mM Hepes, 5 mM Mes at pH 6.0, 10 mM NaCl, 1 mM $CaCl_2$, 100 μM hydrogen peroxide, and 7.6, 8.8, 11.5, 12.7, and 15.7 μM pseudoazurin. The assays were initiated by the addition of cytochrome *c* peroxidase (0.6−1.3 nM).

At the end of each experiment a small amount of potassium ferricyanide was added to the reaction mixture to determine the end point of the reaction. Turnover numbers were calculated from semilog plots of pseudo-first-order progress curves.

Mass Spectrum. Samples of both *P. pantotrophus* LMD 82.5 and recombinant pseudoazurin from *P. pantotrophus* LMD 52.44 were prepared in either 20 mM ammonium acetate at pH 8.0 (for the holo-protein determination) or 5% formic acid (for the apo-protein determination) using a Vivaspin membrane. The samples were freeze-dried. Electrospray mass spectrometry was performed on a Bio-Q quadrupole mass spectrometer equipped with an electrospray ionization source (Micromass, Altrincham, U.K.).

Monomer−Dimer Equilibrium of Pseudoazurin at Different Ionic Strengths. The monomer−dimer equilibrium of pseudoazurin was studied using a molecular-exclusion column. Superdex 75 (30 × 1.0 cm Ø) was equilibrated with 10 mM Hepes at pH 7.0 or 8.0 and 0−1000 mM NaCl. Samples of oxidized pseudoazurin (1 nmol) were prepared in the same ionic strength as the running buffer.

Dipole Moment Calculations. Coordinate files were obtained from http://www.ncbi.nlm.nih.gov. The dipole moment was determined for pseudoazurin isolated from *P. pantotrophus* LMD 82.5 (monomer A, PDB 1ADW, oxidized form), *Achromobacter cycloclastes* (PDB 1BQK, oxidized form; PDB 1BQR, reduced form), and *Alcaligenes faecalis* S-6 (PDB 8PAZ, oxidized form). The dipole moment was also determined for the oxidized plastocyanin from *Phormidium laminosum* (PDB 1BAW), the oxidized amicyanin from *P. denitrificans* (PDB 1AAC), and the oxidized cytochrome c_{550} from *P. pantotrophus* LMD 52.44 (*16*).

The determination was performed using Sybyl (Tripos associates). The charges of the molecule were as follows: +2 or +1, copper; +1, N-terminal amine and lysine side-chain amine; +0.5, arginine NH1 and NH2 atoms; −1, coordinated cysteine S^{γ} atom; and −0.5, paired oxygens of carboxylates (C terminus, glutamate, and aspartate). This calculation ignores charge contributions from the iron and the pyrrole nitrogens in cytochrome c_{550} (which cancel in the Fe^{II} state) and from the ends of α helices (the type-I copper proteins contain very little or no α helix).

Two-Dimensional NMR Titrations. Protein samples were exchanged several times with 10 mM sodium phosphate buffer at pH 5.9, by centrifugation above a Vivaspin membrane with a 10 000 M_r cut off for cytochrome *c* peroxidase or a 5000 M_r cut off for pseudoazurin. The pH of the samples was checked and adjusted, if required, with NaOD (the quoted pH values of the NMR samples were not corrected for the deuterium isotope effect). Two-dimensional heteronuclear NMR spectra were recorded for a 0.2 mM pseudoazurin solution, containing 2 mM $CaCl_2$, 10% D_2O, and an excess of sodium dithionite to maintain the reducing conditions. The reduced pseudoazurin spectrum was assigned by a comparison with that previously published (*33*). Spectra were also recorded after addition of 0.1, 0.2, 0.3, 0.4, and 0.5 equiv of cytochrome *c* peroxidase. After and during addition of peroxidase to pseudoazurin, the samples were flushed with argon to maintain the reducing conditions.

^1H-^{15}N HSQC spectra were recorded at 299 K, on a Bruker Avance DRX 500 spectrometer equipped with a HCN probe and self-shielded triple-axis gradients. Two-dimensional NMR experiments were obtained using a watergate pulse sequence in the TPPI mode. The spectral widths are 7000 Hz for ^1H and 2100 Hz for ^{15}N. A total of 1024 data points in t_2 and 32 transients for each 128 t_1 were used. The NMR spectra were processed with xwinnmr provided by Bruker. ^1H chemical shifts were referenced to the H_2O resonance (4.76 ppm at 299 K), and ^{15}N chemical shifts were referenced indirectly by using the above ^1H reference and gyromagnetic ratios (0.101 329 118).

RESULTS

Properties of Heterologously Expressed Pseudoazurin. The pseudoazurin gene from *P. pantotrophus* LMD 52.44 was isolated by PCR using the LMD 82.5 strain gene sequence to design the primers. Several expression conditions were tested to optimize the amounts of pseudoazurin obtained, and it was found that there was no need to induce the expression by adding IPTG, demonstrating that the gene is constitutive [as already observed by other authors (*34*)]. The recombinant apo pseudoazurin from *P. pantotrophus* LMD 52.44 has an identical M_r (13 343.2 ± 0.2), determined by ESI mass spectrometry, as that isolated from *P. pantotrophus* LMD 82.5 (13 343.2 ± 0.1), a value that is also in agreement with that reported in the literature (13 344 ± 0.5) (*9*) and with that predicted from the amino acid sequence (13 342.3). The M_r of the holo protein was determined to be 13 404.9 ± 0.3, a value in agreement with that predicted from the amino acid sequence with a single copper (13 404.9). These results show that the signal peptide, which directs the protein to the periplasm, was processed correctly and also that the assembly of the protein with copper had occurred normally.

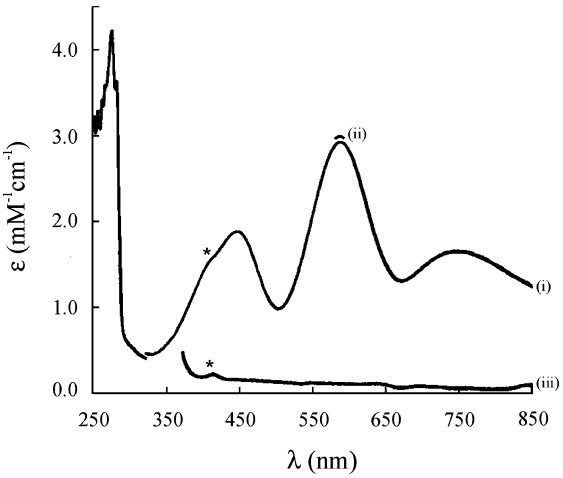

FIGURE 1: UV−visible spectra of pseudoazurin in 10 mM phosphate buffer at pH 7.0, shown as a function of the extinction coefficient. (i) Untreated pseudoazurin from *P. pantotrophus*; (ii) absorbance at 590 nm after complete oxidation with potassium ferricyanide; and (iii) pseudoazurin reduced with sodium dithionite. A small contamination with a cytochrome can be observed (indicated by an asterisk); however, the Soret extinction coefficient is large, and therefore the relative amount is small (0.2% assuming ϵ of 100 mM^{-1} cm^{-1}).

Extinction Coefficient. The total copper and protein concentration and the UV−visible spectra (Figure 1) were determined using a single parent solution of pseudoazurin. The results shown in Table 1 are expressed relative to 1 mM Cu. Copper determination by the colorimetric method using the 2,2′-biquinoline reagent and ICP gave concordant results. On this basis, the extinction coefficient at 590 nm is 3.00 mM^{-1} cm^{-1}. The corresponding protein concentration differed significantly with the method of determination; the one based on determination of free amino group gave a value of 0.94 mol of Cu per mol of protein, whereas that based on the Lowry/Biuret method of protein determination gave 0.81 mol of Cu per mol of protein, and that based on the Bradford method gave 1.89 mol of Cu per mol of protein. The mass determination by mass spectrometry was consistent with a single Cu per mol of protein and showed no sign of the presence of apo protein.

There are changes in the spectrum and therefore in the extinction coefficient with pH (data not shown), with a p*K* value of 7. However, they are very small and give rise to an extinction coefficient of 3.05 mM^{-1} cm^{-1} at pH 6.0 and of 2.96 mM^{-1} cm^{-1} at pH 7.5. Although these are within the error range of the extinction coefficient measurement at pH 7 (Table 1), they were calculated from a single reversible titration and are therefore significant relative to the value of 3.00 at pH 7.

Table 1: Relationship between the Absorbance at 590 nm and the Protein and Copper Content[a]

[protein] (mM)			[copper] (mM)	extinction coefficient (mM^{-1} cm^{-1})
free amino group	Lowry/Biuret	Bradford	2,2′-biquinoline	A_{590nm}
1.06 ± 0.07	1.23 ± 0.1	0.53 ± 0.03	1.00 ± 0.02	3.00 ± 0.04

[a] Values are averages of four independent parallel determinations in the case of copper and free amino-group concentration and of six determinations for the Lowry/Biuret and Bradford methods. The protein concentrations determined by the different methods are expressed relative to the concentration of copper.

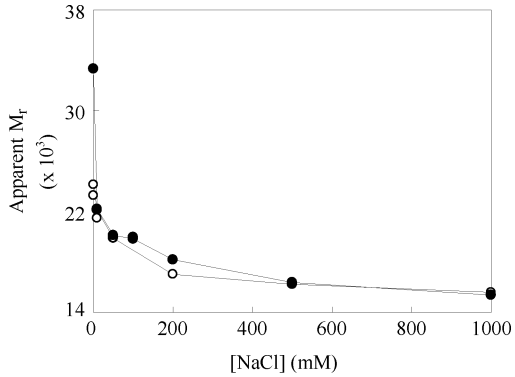

FIGURE 2: Relative molecular mass of pseudoazurin as a function of the NaCl concentration. The relative molecular mass of oxidized pseudoazurin from *P. pantotrophus* (1 nmol) was determined by molecular-exclusion chromatography (Superdex 75), using 10 mM Hepes at pH 8.0 (●) or 7.0 (○) as a running buffer and varying the NaCl concentration between 0 and 1 M.

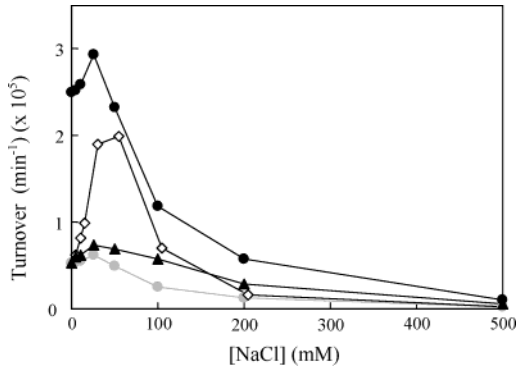

FIGURE 3: Kinetic activity of cytochrome *c* peroxidase as a function of the ionic strength with the different electron donors. The assay was performed in 10 mM Mes, 1 mM $CaCl_2$ at pH 6.0, as described in the Materials and Methods. The electron donors used were pseudoazurin from *P. pantotrophus* (●), cytochrome c_{550} from *P. pantotrophus* LMD 52.44 (▲) and horse heart cytochrome *c* (○). The experiments were performed with two different batches of cytochrome *c* peroxidase, and the activity with horse heart cytochrome *c* was used to normalize the two experiments. The pseudoazurin turnover numbers normalized for the turnover number of cytochrome c_{550} at 0 mM NaCl are also shown in gray (this is to allow for a comparison of the trends).

Monomer−Dimer Equilibrium. The relative molecular mass of pseudoazurin was measured at different ionic strengths and at two different pH values (7.0 and 8.0) by molecular-exclusion chromatography (Figure 2). At low ionic strength, the M_r was approximately 33 000, and this value decreased with an increasing ionic strength to reach 15 500 at 1.0 M NaCl. This pattern was similar for both pH values (7.0 and 8.0), and we interpret this to represent a monomer−dimer equilibrium that is dependent on the ionic strength.

Pseudoazurin as an Electron Donor to Cytochrome c Peroxidase. The kinetic assay used was a modified version of that published previously in Gilmour et al. (*4*). Higher concentrations of electron donors were used, and therefore the concentration of hydrogen peroxide was increased to achieve complete oxidation.

Because of the high K_m and the difficulty of collecting data at very high substrate concentrations, the kinetic parameters of the maximal turnover number (TN) and K_m for pseudoazurin as an electron donor to cytochrome *c* peroxidase could not be determined with accuracy. Estimates were a K_m of 70 μM and a TN_{max} of 10 950 s^{-1}.

The ionic strength dependence of the kinetic activity was studied, and the profile obtained is shown in Figure 3, which also includes the values for cytochrome c_{550} and horse heart cytochrome *c* determined under the same conditions as pseudoazurin. Turnover numbers for pseudoazurin are higher than those for the two cytochromes. The oxidation of all electron donors was dependent on the ionic strength. In all cases, the curve has a peak of activity, which is most pronounced for horse cytochrome *c* and occurs at about 50 mM NaCl.

Dipole Moment Calculation. The dipole moment was calculated for the pseudoazurins of *P. pantotrophus*, *A. cycloclastes*, and *A. faecalis*, the plastocyanin of *P. laminosum*, and the amicyanin from *P. pantotrophus.* The results are compared in Table 2 with those obtained for cytochrome c_{550} (*16*) and by Koppenol et al. (*14*) for horse cytochrome *c*.

Table 2: Dipole Moments of Pseudoazurins and Related Proteins

organism	protein	redox state	net charge	dipole moment (Debye)
P. pantotrophus LMD 82.5	pseudoazurin	oxidized	−4	704
		reduced[a]	−5	651
A. cycloclastes	pseudoazurin	oxidized	+1	518
		reduced[b]	0	419
A. faecalis S-6	pseudoazurin	oxidized	−1	498
P. laminosum	plastocyanin	oxidized	−3	388
P. pantotrophus LMD 82.5	amicyanin	oxidized	−3	466
P. pantotrophus LMD 52.44	cytochrome c_{550}	reduced[c]	−9	965
horse	cytochrome *c*	reduced	+6	299

[a] Determined using the coordinates of the oxidized form with a charge of +1 on the copper. [b] Determined using the coordinates of the reduced form. [c] Determined using the coordinates of the oxidized form with no net charge on the haem group.

Mapping of the Interaction Surface of Pseudoazurin with Cytochrome c Peroxidase. A portion of the pattern of perturbation of amide nitrogen and amide proton resonances of the pseudoazurin in the presence of cytochrome *c* peroxidase is shown in Figure 4. The titration could only be analyzed up to a cytochrome *c* peroxidase/pseudoazurin ratio of 0.3; beyond that, reliable identification was precluded by peak

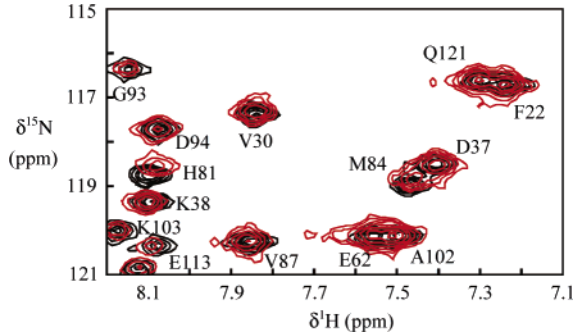

FIGURE 4: Spectral region of the overlaid ^{1}H-^{15}N heteronuclear NMR spectra of free pseudoazurin (black) and pseudoazurin in the presence of 0.3 M equiv of cytochrome *c* peroxidase (red).

broadening. At this molar ratio, it was observed that some resonances shift and also become broader (Figure 4), indicating that the exchange between the free and the bound states of pseudoazurin is "fast" on the chemical-shift time scale.

The ^{15}N chemical-shift variations had a maximum of 0.33 ppm, while the ^{1}H chemical-shift variation did not exceed 0.11 ppm. However, because the extent of chemical shift is proportional to the extent of binding, our values will fall somewhere short of the full chemical shifts, if binding had been complete. In related experiments with plastocyanins, Crowley et al. (*17*) have extrapolated their data to complete binding and used a combination of the perturbation of a nitrogen and its associated proton to present the results. Because we have not reached 50% occupancy in these experiments, we have not attempted this extrapolation to complete occupancy, and the shifts are presented in Figure 5 as raw results.

In the presentation of the results, a threshold is usually set and results above that threshold are presented as binding shifts. For example, in Morelli et al. (*35*), a threshold of 0.1 ppm was set for ^{15}N and a threshold of 0.02 ppm, for ^{1}H. If we apply these thresholds to our data, the 12 surface residues in dark gray in Figure 6 are identified as shifted by binding (L8, F18, D37, S58, K59, E62, S63, Y64, T79, H81, M84, and K109). There are three further large binding shifts in Figure 5 for residues 88, 89, and 102, and these are buried residues not visible in Figure 6. However, we can reasonably argue that these thresholds are too high for a titration that has reached only 0.3 M binding proportions. If we apply thresholds of half of these values, the residues in light gray are included as shifted by binding (Figure 6) and, in total, 45 residues are identified as being perturbed because of the binding of peroxidase. These can be divided into several categories depending on their location.

A total of 18 of the 45 residues affected by binding (N9, M16, D37, K38, S39, E43, A44, K46, K59, I60, N61, K77, T79, H81, G83, M84, K109, and K110) are located on the *"front" face* of the pseudoazurin, centered on His81 and the dipole vector (Figure 6A). The six lysines form a ring of positive charge around the perimeter of the front face. A total of 6 residues of the group of 18 (D37, K59, T79, H81, M84, and K109) exhibit larger effects (above 0.1 for ^{15}N and 0.02 for ^{1}H) and only 4 (S39, A44, G83, and K110) are not conserved among the pseudoazurins.

A number of *buried residues* show chemical-shift variation in their NH resonance and include M86 (a copper ligand

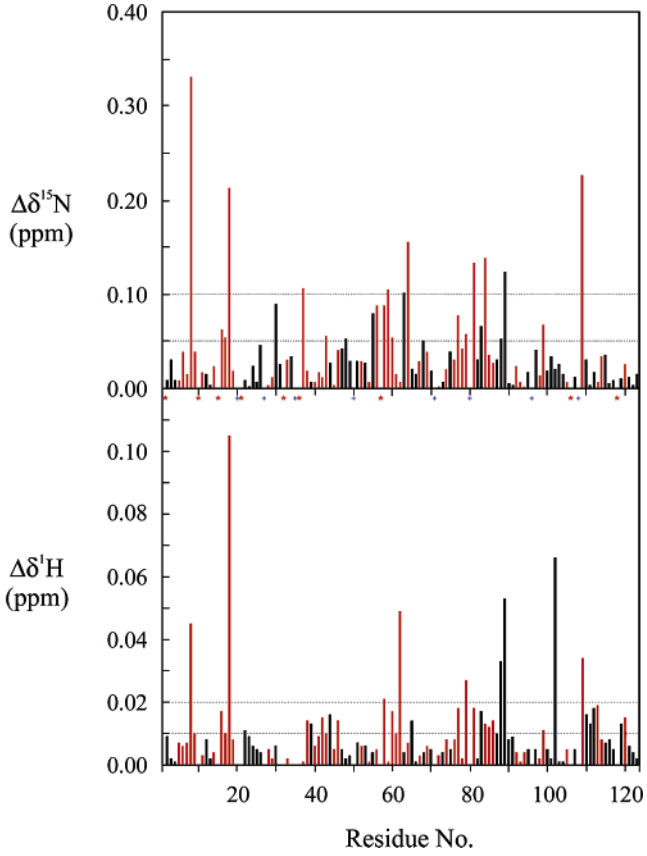

FIGURE 5: ^{1}H and ^{15}N chemical-shift variations observed on the NH of pseudoazurin residues, in heteronuclear NMR experiments in the presence of 0.3 equiv of cytochrome *c* peroxidase. An asterisk indicates nonassigned residues (1, 10, 15, 21, 32, 36, 57, 106, and 118), and a plus sign indicates nonobservable proline residues (20, 27, 35, 50, 71, 80, 96, and 108). The red bars correspond to residues conserved between the pseudoazurins from *P. pantotrophus*, *P. denitrificans*, *A. cycloclastes* and *A. faecalis*. Variations were both positive and negative. The absolute value is shown here.

buried under the front face) and residues that are located nearby (G85, V87, G88, and L89).

Surface residues not at the front face include a large number of residues affected by binding that are situated just back from the front face and appear as a rim of gray in parts C and D of Figure 6. The significance of these residues is discussed below. No residues affected by binding are found at the "back" of the molecule (Figure 6B).

DISCUSSION

Isolation of the Pseudoazurin Gene from P. pantotrophus LMD 52.44. Despite strenuous efforts under different growth conditions, we could not achieve pseudoazurin expression for the *P. pantotrophus* LMD 52.44 strain. However, the isolated gene was found to be identical to that from *P. pantotrophus* LMD 82.5 (*24*). This is consistent with the proposal that these two strains do belong to the same species (*19*, *36*) and the fact that the amino acid sequences of the respective cytochrome c_{550} differ in just one position (*36*). Our inability to detect pseudoazurin in the periplasm of *P. pantotrophus* LMD 52.44 could be due to a low level of expression or to a mutation in its promoter region. The expression of pseudoazurin, as well as of cytochrome *c* peroxidase, is controlled by a FnrP factor (*24*, *37*, *38*). Because we find that cytochrome *c* peroxidase is induced

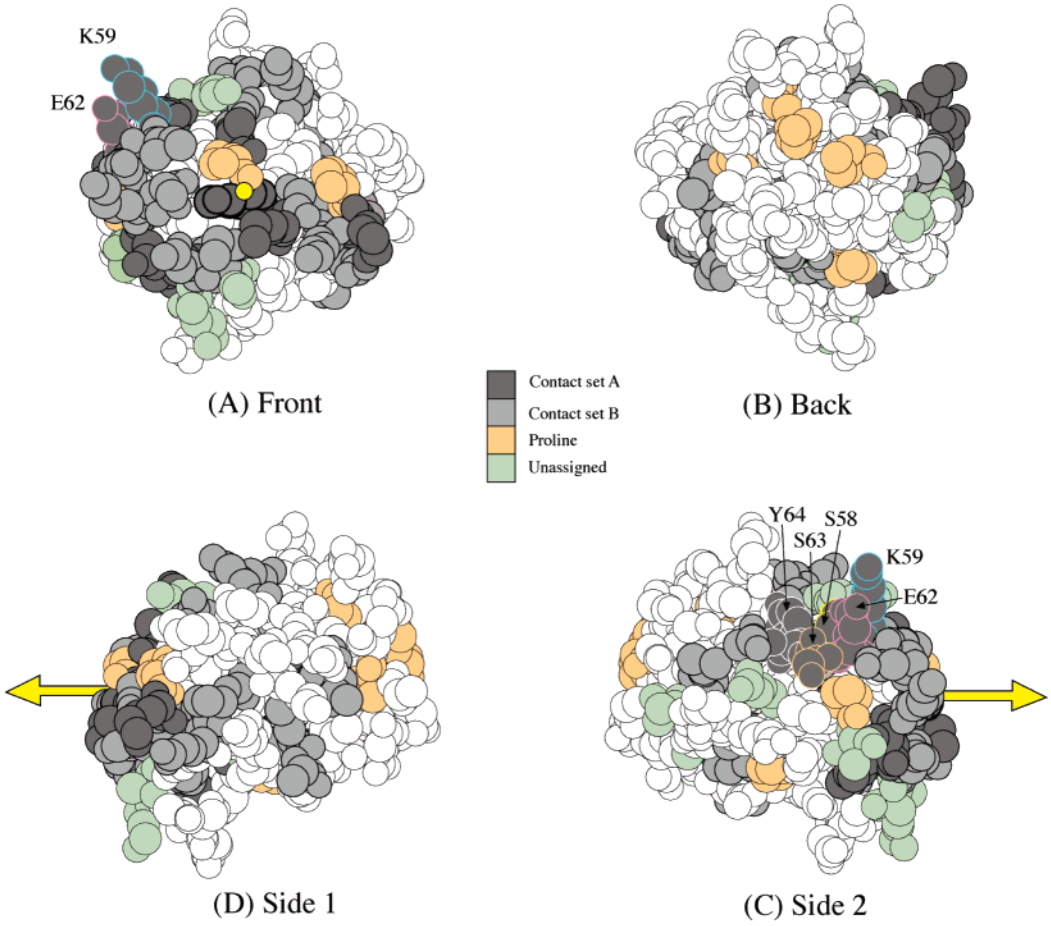

FIGURE 6: Mapping of chemical-shift perturbation on the surface of pseudoazurin. Different views are shown of the surface of the pseudoazurin from *P. pantotrophus* rendered by the molecular graphics program MacImdad. The front view (A) is defined by the presence of His81 (shown in bold outline) and is centered on the dipole vector, which is perpendicular to the plane of the page (small yellow circle). Contact set A (dark gray circles) include those residues that experience chemical-shift perturbation in the presence of 0.3 mol of cytochrome *c* peroxidase of greater than 0.1 ppm for ^{15}N or 0.02 ppm for ^{1}H. Contact set B (light gray circles) are those additional residues that experience chemical-shift perturbation of greater than 0.05 ppm for ^{15}N or 0.01 ppm for ^{1}H. Proline residues (orange) cannot be observed because they lack an amide proton. The resonances of unassigned residues (green) are present in the chemical-shift perturbation map but are poorly resolved from neighboring resonances. C and D show the side views, which are the result of the rotation of A by ±90° in a horizontal plane, perpendicular to the plane of the page. The dipole vectors are shown as yellow arrows. The residues K59 and E62 are shown outlined in blue and red, respectively, in A and again in D. The lysine NZ atom is 4.5 Å from the glutamate OE2 atom. Neighbors (Y64, S63, and S58) of this charge pair, which are also strongly perturbed on binding to the peroxidase and are referred to in the Discussion, are shown outlined in white, yellow, and purple, respectively, in D to distinguish them clearly.

under low oxygen concentrations but that the pseudoazurin is not, a mutation in the pseudoazurin promoter seems more likely than a mutation in FnrP. A determination of the sequence of the upstream region of the pseudoazurin gene could test this hypothesis.

Because we have not found conditions for expression of pseudoazurin in the LMD 52.44 strain, it could be argued that we are studying a nonphysiological interaction between the cytochrome *c* peroxidase of *P. pantotrophus* LMD 52.44 and its cloned pseudoazurin. However, we know that the cytochrome *c* peroxidase and pseudoazurin of *P. pantotrophus* LMD 82.5 are physiological reactants and that the pseudoazurins from the two *P. pantotrophus* strains are identical. In addition, the cytochrome *c* peroxidases from the two strains show an identical M_r value by mass spectrometry. This argues for a simple loss of pseudoazurin promoter function in the LMD 52.44 strain, which does not have consequences for viability because the cytochrome c_{550} acts as an alternative electron donor.

Extinction Coefficient. The molecular mass of the recombinant pseudoazurin from *P. pantotrophus* LMD 52.44 is identical to the protein from *P. pantotrophus* LMD 82.5, and we propose that they are the same protein. However, the reported extinction coefficient (590 nm) for the pseudoazurin from *P. pantotrophus* 82.5 was 1.36 mM^{-1} cm^{-1} (*9*), much lower than the value of 3.00 mM^{-1} cm^{-1} obtained here for the recombinant protein from *P. pantotrophus* 52.44. A value of 3.00 mM^{-1} cm^{-1} was also obtained in our study for pseudoazurin prepared from *P. pantotrophus* LMD 82.5.

Variation in copper occupancy would lead to different values for an extinction coefficient. We are confident that the copper occupancy in our preparation is close to 1. A value of 0.94 can be calculated from the values in Table 1 using the determination of amino groups as the measure of protein concentration. It is also supported by the mass spectrometric analysis of the holo protein, which shows a species of M_r = 13 404.9 and no peak corresponding to the apo protein (which would have indicated partial-site occupancy). It is clear from Table 1 that the method of protein determination markedly affects the results. In our study, the Bradford method [used by Moir et al. (9)] underestimated the protein concentration.

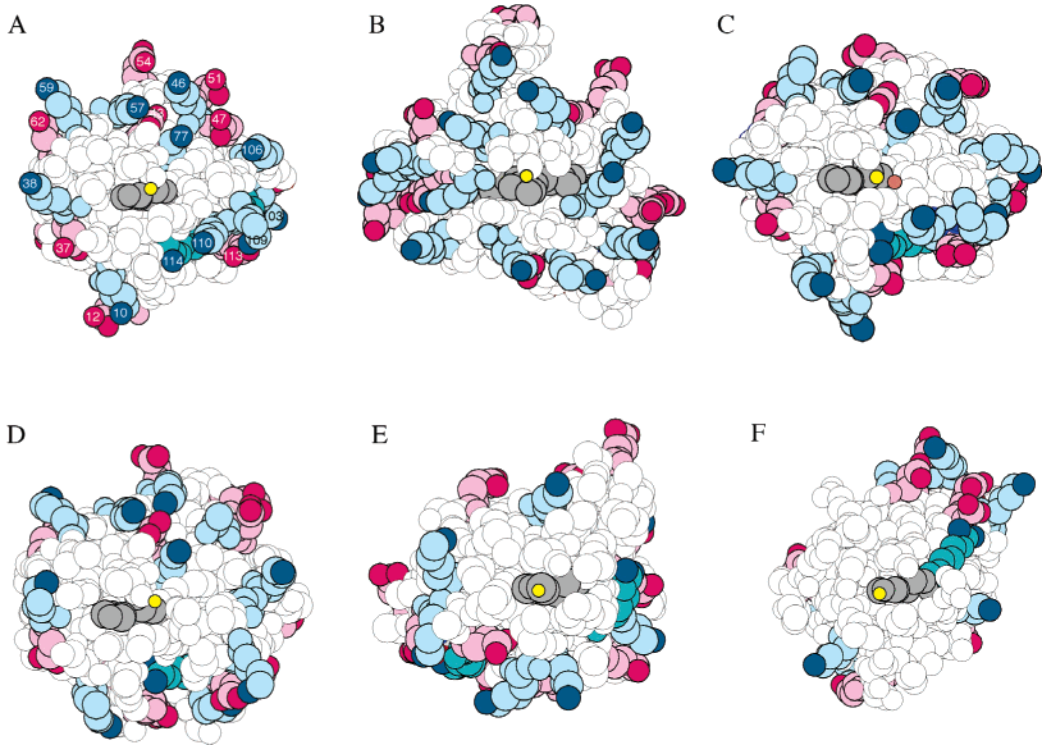

FIGURE 7: Dipole vector and the charged residues of the front face of pseudoazurin and related proteins. Front surface views of the proteins are rendered in MacImdad. The front view is defined by the presence of the exposed histidine (H81 in *P. pantotrophus* pseudoazurin) (grey circles) and is centered on the dipole vector (small yellow circle). The small additional orange circle in C represents the position of the dipole vector for the reduced form of *A. cycloclastes* pseudoazurin. In all cases, lysine side chains are light blue, and lysine NZ atoms are dark blue; arginine side chains are turquoise, and arginine NH1 and NH2 atoms are dark blue; aspartate and glutamate side chains are pink, and aspartate OD1 and OD2 and glutamate OE1 and OE2 atoms are red. The coordinate files are for the oxidized forms of the pseudoazurins and the cytochrome c_{550}. (A) *P. pantotrophus* LMD 82.5 pseudoazurin (PDB 1ADW, monomer A). (B) *P. pantotrophus* LMD 52.44 cytochrome c_{550} (see ref *16*). (C) *A. cycloclastes* pseudoazurin (PDB 1BQK). (D) *A. faecalis* pseudoazurin (PDB 8PAZ). (E) *P. pantotrophus* amicyanin (PDB 1AAC). (F) *P. laminosum* plastocyanin (PDB 1BAW).

Our revised value of 3.00 mM^{-1} cm^{-1} is in line with the values obtained for other pseudoazurins [2.9 mM^{-1} cm^{-1} for *A. faecalis* S-6 (*39*) and 3.7 mM^{-1} cm^{-1} for *A. cycloclastes* (*40*)]. The new value will require some revision of the kinetic parameters of nitrite reductase (*10*) and hydroxylamine oxidase (*41*).

Pseudoazurin as an Electron Donor to Cytochrome c Peroxidase. The K_m determined was higher than 50 μM, which is in agreement with that reported in the literature (*13*). However, in that study, the extinction coefficient used was not the correct one and the assay did not use preactivated CCP. Pseudoazurin has a higher K_m than that reported for cytochrome c_{550} (13 μM), a value also determined in a curve that had not approached saturation (*4*). Although the K_m is high, the protein concentrations in the periplasm of, for example, *P. pantotrophus* LMD 82.5 are likely to match or exceed it (*9*).

The turnover numbers for pseudoazurin are higher than those for cytochrome c_{550}. If the two proteins bind at the same site, then the preference of the enzyme will be determined by the prevailing donor concentrations and the K_m value.

Binding Surface on Pseudoazurin for Interaction with Cytochrome c Peroxidase. The use of heteronuclear NMR spectroscopy allows the detection of small perturbations in the environment of the amide nitrogens of a protein labeled with ^{15}N when the protein binds to a redox partner. These small perturbations may be a primary effect of the change in the chemical environment if the amino acid is present in the interface between the two proteins, but secondary effects are also possible as a result of small adjustments of the polypeptide chain and side chains in the bound complex. The perturbations may result in a shift in the amide nitrogen resonance itself, the resonance of its associated proton, or both. The results of Figure 5 show the pattern of cross perturbation that was achieved in the case of the interaction of pseudoazurin and cytochrome *c* peroxidase.

It is clear from Figure 6A that residues that are affected by binding in the presence of the peroxidase populate the pseudoazurin face centered on His81 and the dipole moment. This is consistent with the proposal that it is this surface that is involved in binding to the cytochrome *c* peroxidase, allowing electron transfer to occur near His81. Kukimoto et al. reached the same conclusion for the pseudoazurin from *A. faecalis* based on the effects of mutation of individual lysines on the activity with nitrite reductase (*42*).

However, many of the pseudoazurin residues that experience a binding shift are situated just back from the rim of lysines that encircle the front face of the molecule. We propose that these are secondary effects and that they may be particularly evident in pseudoazurin because of the striking pairings that exist between the lysines that encircle His81 and acidic residues. Many of these pairings are apparent from Figure 7, and include K59−E62, K57−E43−K77, K46−E47−K106, K38−D37, K12−E12, K109−E113, and R112−D116. Only the latter two pairings have separation distances within 3 Å in the crystallographic structure, but given the flexibility of the lysine side chains, there is at least a

possibility that electrostatic interactions also occur in the others. Our proposal is that the relationship of these lysines to their paired acidic residues is subtly altered when pseudoazurin binds against the broad negative surface of the peroxidase. Such readjustments of lysines would be expected to have a secondary effect on the environment of the paired acidic residues and the residues in their immediate vicinity. A striking example of this is K59, which is associated with E62. The amide of the latter is strongly shifted by binding (Figure 5), but the amides of the neighboring residues S58, S63, Y64, and T65 are also strongly affected (Figure 6D). The E62 is just below the rim of the front face, and the serines and tyrosine are even further back (Figure 6D). It is this type of effect that leads to the distribution of residues affected by binding apparent in parts C and D of Figure 6. A similar effect can explain the chemical-shift variation observed for the NH resonance of residues L99, A102, A111, R112, and E113 and the effect on F56, a residue that is located next to a lysine residue (K57), the NH resonance of which could not be assigned.

We conclude therefore that pseudoazurin binds to cytochrome *c* peroxidase at its front face. This face includes the site of electron transfer, which is surrounded by a hydrophobic patch, which in turn is surrounded by a ring of lysines. Because of the frequent association of this set of lysines with acidic residues just back from the front face, secondary binding shifts are observed in those acidic residues and their neighbors.

Pseudoazurin and General Theories of Biological Electron Transfer. A feature of the current models of the biological electron transfer is the idea of a fluid-encounter complex consisting of a collection of electrostatically preorientated configurations of a small redox protein with its partner redox enzyme (*17*, *18*, *43*). Lateral mobitlity allows a "search" for an optimal orientation, which facilitates electron transfer. Although global electrostatic forces are implicated in preorientation, the final electron-transfer complex is stabilized by hydrophobic interactions. Indeed, in contrast to an earlier emphasis on the formation of electrostatic linkages across the interface of the complex, it may be important to avoid such links to maintain fluidity and transiency during the encounter. The nonspecific nature of the hydrophobic interactions is consistent with the pseudospecificity (*1*) observed in biological electron transfers, whereby one small redox protein may interact with several redox enzymes.

If we turn from the general case to the specific case of the pseudoazurin studied here, a striking feature is the orientation of the very large dipole moment. This vector, which is rooted in the center of mass, leaves the protein at the histidine, which is coordinated to the buried copper (Figure 7A). It is this histidine that is proposed to be near the site of electron transfer. In this respect, the pseudoazurin resembles the cytochrome c_{550} from the same source (Figure 7B), the dipole moment of which leaves the protein at the exposed haem edge. We should keep in mind that the dipole moment is not determined by the total net charge but by the charge distribution. Pseudoazurin and cytochrome c_{550} have net charges of -4 and -9, respectively, and yet share the feature of a positive dipole vector situated at their electron-transfer sites. Also, the positioning of the negative charge behind the binding surface is as influential as the positioning of the positive charge at the front (*14*, *42*, *44*). Thus, although the pseudoazurins have a striking "ring of lysines" around their front face (parts A, C, and D of Figure 7), the plastocyanin from *P. laminosum* does not, yet it has a dipole moment, which is positioned precisely above the key histidine (Figure 7F) and which has a magnitude greater than that for mitochondrial cytochrome *c* (Table 2).

We conclude that the large dipole moment in pseudoazurin may allow preorientation in the encounter complex with the cytochrome *c* peroxidase. Our additional observation is that the lysines, which form a ring or rim around the front face of pseudoazurin, often have a neighboring compensating charge just back from the rim in the form of aspartate and glutamate side chains (a feature also noted by Kukimoto et al. (*42*)]. We have found that the amide resonances of many of these residues experience contact shifts on binding cytochrome *c* peroxidase and propose that this is a secondary effect transmitted through the lysines. The presence of these acidic residues may limit the ability of the long lysine side chains to form salt links with the peroxidase across the interface. Formation of such salt links would run the risk of locking the SRP in an immobile and unproductive state on the broad negative surface of the peroxidase. Thus, we see the presence of the rim of lysines with its associated substructure of acidic residues as being essential for optimizing electrostatic retention and preorientation in the encounter, without compromising mobility.

The question remains how we can explain the magnitude of the dipole moments of pseudoazurin and cytochrome c_{550}, which are 2−3-fold greater than those for mitochondrial cytochromes *c*. Larger is not necessarily better in this respect because too large a dipole moment may result in too strong an association being made that is unable to dissociate rapidly. Relevant here, may be the lipid composition of the mitochondrial membrane, which contains 25% of the negatively charged phospholipid cardiolipin (*45*). Too large a dipole moment might lead to a sequestering of mitochondrial cytochrome *c* on the inner-membrane surface. This is less of a problem in the bacterial case, where the cell membrane contains only 3% cardiolipin (*46*).

Ionic Strength Dependence of Steady-State Activity. Increasing ionic strength may influence the rate of association, preorientation within the encounter complex, stability of the reactive complex, and rate of dissociation of the products. Thus, the interpretation of curves such as that of the ionic strength dependence of steady-state activity (Figure 3) is complex. The rise in activity with ionic strength that we observe with the nonphysiological donor horse cytochrome *c* is correlated with a 3-fold decrease in the binding affinity (*5*). We have argued that this may be due to too tight an association at low ionic strengths, which leads either to an encounter complex frozen in an immobile form that is unable to seek out the reactive configuration or to poor rates of dissociation of the product. Presteady-state kinetics may distinguish these alternatives. Either way, horse cytochrome *c* has not been "educated" during evolution by the binding surface of cytochrome *c* peroxidase and becomes trapped on the surface by formation of strong but inappropriate electrostatic forces. Thus, although we believe electrostatics are crucial in preorientation leading to rate enhancement, they must be managed in such a way that mobility is maintained. Herein lies the importance of the effective combination of the dipole moment and the compensating negative charges.

In the low ionic strength range, neither cytochrome c_{550} nor pseudoazurin show much variation in activity (Figure 3) nor is there much reduction in the binding affinity as the ionic strength is raised (Pauleta et al., unpublished results).

The shallow change in activity with ionic strength in cytochrome c_{550} (and, to a lesser extent, pseudoazurin) may be significant physiologically. As a soil bacterium, the periplasm of *P. pantotrophus* will be exposed to a range of ionic strengths (unlike the constant ionic strength environment of a chloroplast or a mitochondrion), and it will be important that the rates of electron transfer are maintained in these different conditions.

Monomer−Dimer Equilibrium. There is some discrepancy between the predicted relative molecular mass for the monomer (M_r = 13 406) and dimer (M_r = 26 812) and the values observed (M_r = 15 500 and 33 000, respectively). However, molecular-exclusion behavior is influenced by shape as well as size, and pseudoazurin is not a simple spherical shape. The Stokes volume for the monomer can be calculated (the volume it would occupy during molecular exclusion) and corresponds to an M_r of approximately 15 000, which is consistent with the value obtained. Applying the same principle to the dimer, an M_r of approximately 30 000 can be calculated, again in agreement with the value obtained.

Pseudoazurin isolated from different sources was found to be a monomer in both the oxidized and the reduced forms (*47*−*49*), but *P. pantotrophus* pseudoazurin is an exception that exhibits monomer−dimer equilibrium in the oxidized form but not in the reduced form (*1*, *33*). This equilibrium was studied (Figure 2) and shown to be ionic-strength- and not pH-dependent (between pH 7−8). In a previous study (*1*), both ionic strength and pH were varied simultaneously, and it was found that a pH of 7.0 and a *I* of 44.4 mM favored the monomer, while a pH of 5.0 and a *I* of 14 mM favored the dimer. In light of our results, it is likely to be the lower ionic strength in the latter conditions that leads to the stronger association.

The relationship between the individual monomer dipole moments and the orientation of the monomers in the crystallographic dimer (*1*) is shown in Figure 8. It is clear that the orientation is such that the dipoles oppose each other in the dimer; the opposing dipoles may indeed contribute to dimer stability. A similar behavior was observed for *P. pantotrophus* cytochrome c_{550} (*16*). This, however, raises the question of why, if electrostatic preorientation using the dipole moment of the monomer is so important, the dimer exists at all. We should note that, as far as the reaction with cytochrome *c* peroxidase is concerned, this question does not arise because the substrate of this enzyme is the monomeric reduced pseudoazurin. Indeed, we might be tempted to propose that dimerization in the oxidized state is a way of preventing either the association of the oxidized form of pseudoazurin with the membrane or the formation of dead-end product complexes with the cytochrome *c* peroxidase. However, a weakness of this argument is that the pseudoazurin does require reduction and presumably must preorientate and bind to the bc_1 complex or a soluble redox enzyme in the monomeric oxidized state. The dimer would seem to compromise this process. It therefore remains a puzzling feature of many small bacterial redox proteins that they are dimers.

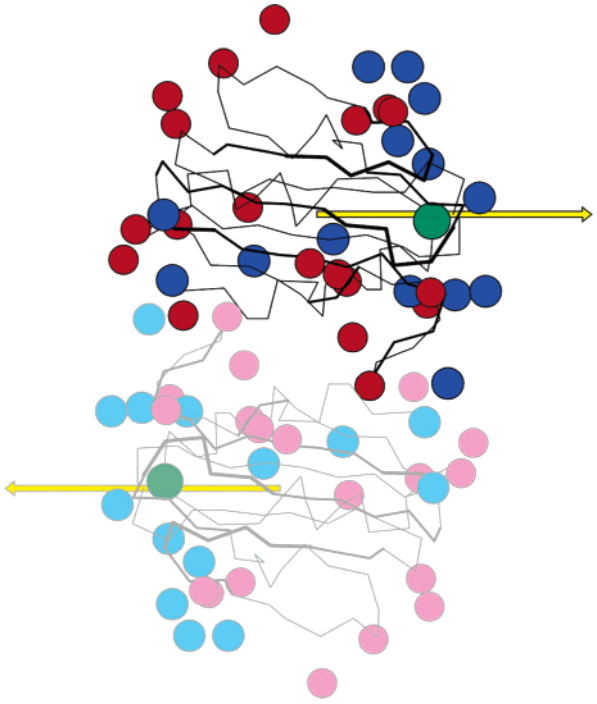

FIGURE 8: Charge distribution of the pseudoazurin dimer. The dimer of pseudoazurin from *P. pantotrophus* LMD 82.5 (PDB 1ADW) is shown rendered in MacImdad. The polypeptide chain is represented by linked α-carbon atoms. Lysine NZ atoms and the N-terminal α amine are shown in blue; aspartate OD1 and glutamate OE1 atoms and the C-terminal OXT atom are shown in red. The copper is green. The dipole vectors (calculated for each individual monomer) are shown as yellow arrows rooted in the center of mass and orientated in the plane of the page.

CONCLUSIONS

The positive vector of the very large dipole moment of pseudoazurin from *P. pantotrophus* LMD 52.44 is positioned at the putative electron-transfer site, His81, and is proposed to be instrumental in preorientation of the molecule against the negatively charged cytochrome *c* peroxidase. The NMR resonances of residues on the face of the protein containing the histidine are perturbed by binding to the peroxidase. These residues include a ring of lysines that are paired with acidic residues just back from the rim. We propose that these acidic residues moderate the electrostatic influence of the lysines and so ensure that specific charge interactions do not form across the interface with the peroxidase.

REFERENCES

1. Williams, P. A., Fulop, V., Leung, Y. C., Chan, C., Moir, J. W., Howlett, G., Ferguson, S. J., Radford, S. E., and Hajdu, J. (1995) Pseudospecific docking surfaces on electron-transfer proteins as illustrated by pseudoazurin, cytochrome c_{550}, and cytochrome cd_1 nitrite reductase, *Nat. Struct. Biol. 2*, 975−982.
2. Ellfolk, N., Rönnberg, M., and Österlund, K. (1991) Structural and functional features of *Pseudomonas* cytochrome *c* peroxidase, *Biochim. Biophys. Acta 1080*, 68−77.
3. De la Rosa, M. A., Navarro, J. A., Díaz-Quintana, A., De la Cerda, B., Molina-Heredia, F. P., Balme, A., Murdoch, P. S., Díaz-Moreno, I., Durán, R. V., and Hervás, M. (2002) An evolutionary analysis of the reaction mechanisms of photosystem I reduction by cytochrome c_6 and plastocyanin, *Bioelectrochem. Bioenerg. 55*, 41−45.
4. Gilmour, R., Goodhew, C. F., Pettigrew, G. W., Prazeres, S., Moura, J. J., and Moura, I. (1994) The kinetics of the oxidation of cytochrome *c* by *Paracoccus* cytochrome *c* peroxidase, *Biochem. J. 300*, 907−914.

5. Pettigrew, G. W., Goodhew, C. F., Cooper, A., Nutley, M., Jumel, K., and Harding, S. E. (2003) The electron-transfer complexes of cytochrome *c* peroxidase from *Paracoccus denitrificans*, *Biochemistry 42*, 2046−2055.
6. Pearson, I. V., Page, M. D., van Spanning, R. J., and Ferguson, S. J. (2003) A mutant of *Paracoccus denitrificans* with disrupted genes coding for cytochrome c_{550} and pseudoazurin establishes these two proteins as the in vivo electron donors to cytochrome cd_1 nitrite reductase, *J. Bacteriol. 185*, 6308−6315.
7. Sutton, V. R., Stubna, A., Patschkowski, T., Munck, E., Beinert, H., and Kiley, P. J. (2004) Superoxide destroys the $[2Fe-2S]^{2+}$ cluster of FNR from *Escherichia coli*, *Biochemistry 43*, 791−798.
8. Crack, J., Green, J., and Thomson, A. J. (2004) Mechanism of oxygen sensing by the bacterial transcription factor fumarate−nitrate reduction (FNR), *J. Biol. Chem. 279*, 9278−9286.
9. Moir, J. W., Baratta, D., Richardson, D. J., and Ferguson, S. J. (1993) The purification of a cd_1-type nitrite reductase from, and the absence of a copper-type nitrite reductase from, the aerobic denitrifier *Thiosphaera pantotropha*; the role of pseudoazurin as an electron donor, *Eur. J. Biochem. 212*, 377−385.
10. Richter, C. D., Allen, J. W. A., Higham, C. W., Koppenhöfer, A., Zajicek, R. S., Watmough, N. J., and Ferguson, S. J. (2002) Cytochrome cd_1, reductive activation and kinetic analysis of a multifunctional respiratory enzyme, *J. Biol. Chem. 277*, 3093−3100.
11. Berks, B. C., Baratta, D., Richardson, D. J., and Ferguson, S. J. (1993) Purification and characterization of a nitrous-oxide reductase from *Thiosphaera pantotropha*—Implications for the mechanism of aerobic nitrous-oxide reduction, *Eur. J. Biochem. 212*, 467−476.
12. Moir, J. W. B., and Ferguson, S. J. (1994) Properties of a *Paracoccus denitrificans* mutant deleted in cytochrome c_{550} indicate that a copper protein can substitute for this cytochrome in electron transport to nitrite, nitric oxide, and nitrous oxide, *Microbiology 140*, 389−397.
13. Richardson, D. J., and Ferguson, S. J. (1995) Competition between hydrogen peroxide and nitrate for electrons from the respiratory chains of *Thiosphaera pantotropha* and *Rhodobacter capsulatus*, *FEMS Microbiol. Lett. 132*, 125−129.
14. Koppenol, W. H., et al. (1991) The dipole moment of cytochrome *c*, *Mol. Biol. Evol. 8*, 545−558.
15. Koppenol, W. H., and Margoliash, E. (1982) The asymmetric distribution of charges on the surface of horse cytochrome *c*, *J. Biol. Chem. 257*, 4426−4437.
16. Pettigrew, G. W., Gilmour, R., Goodhew, C. F., Hunter, D. J., Devreese, B., Van Beeumen, J., Costa, C., Prazeres, S., Krippahl, L., Palma, P. N., Moura, I., and Moura, J. J. (1998) The surface-charge asymmetry and dimerisation of cytochrome c_{550} from *Paracoccus denitrificans*—Implications for the interaction with cytochrome *c* peroxidase, *Eur. J. Biochem. 258*, 559−566.
17. Crowley, P. B., and Ubbink, M. (2003) Close encounters of the transient kind: Protein interactions in the photosynthetic redox chain investigated by NMR spectroscopy, *Acc. Chem. Res. 36*, 723−730.
18. Hart, S. E., Schlarb-Ridley, B. G., Delon, C., Bendall, D. S., and Howe, C. J. (2003) Role of charges on cytochrome *f* from the cyanobacterium *Phormidium laminosum* in its interaction with plastocyanin, *Biochemistry 42*, 4829−4836.
19. Rainey, F. A., Kelly, D. P., Stackebrandt, E., Burghardt, J., Hiraishi, A., Katayama, Y., and Wood, A. P. (1999) A re-evaluation of the taxonomy of *Paracoccus denitrificans* and a proposal for the combination *Paracoccus pantotrophus* comb. nov., *Int. J. Syst. Bacteriol. 49* (part 2), 645−651.
20. Robertson, L. A., and Kuenen, J. G. (1983) *Thiosphaera pantotropha* gen. nov. sp. nov., a facultatively anaerobic, facultatively autotrophic sulphur bacterium, *J. Gen. Microbiol. 129*, 2847−2855.
21. Kuenen, J. G., Robertson, L. A., and Tuovinen, O. H. (1992) in *The prokaryotes—A handbook on the biology of bacteria: Ecophysiology, isolation, identification, applications* (Balows, A., Trüper, H. G., Dworkin, M., Harder, W., and Schleifer, K. H., Eds.) pp 2638−2647, Springer-Verlag, Heidelberg, Germany.
22. Goodhew, C. F., Wilson, I. B., Hunter, D. J., and Pettigrew, G. W. (1990) The cellular location and specificity of bacterial cytochrome *c* peroxidases, *Biochem. J. 271*, 707−712.
23. Sambrook, J., Fritsch, E. F., and Maniatis, T. (1989) *Molecular Cloning: A Laboratory Manual*, 2nd ed., Cold Spring Harbor, New York.
24. Leung, Y. C., Chan, C., Reader, J. S., Willis, A. C., van Spanning, R. J., Ferguson, S. J., and Radford, S. E. (1997) The pseudoazurin gene from *Thiosphaera pantotropha*: Analysis of upstream putative regulatory sequences and overexpression in *Escherichia coli*, *Biochem. J. 321*, 699−705.
25. Hunter, D. J. B., Brown, K. R., and Pettigrew, G. W. (1989) The role of cytochrome-*c*4 in bacterial respiration—Cellular location and selective removal from membranes, *Biochem. J. 262*, 233−240.
26. Hanna, P. M., Tamilarasan, R., and McMillin, D. R. (1988) Cu(I) analysis of blue copper proteins, *Biochem. J. 256*, 1001−1004.
27. Habeeb, A. F. S. A. (1966) Determination of free amino groups in proteins by trinitrobenzenesulfonic acid, *Anal. Biochem. 14*, 328−336.
28. Means, G. E., and Feeney, R. E. (1971) *Chemical Modification of Proteins*, Holden-Day, San Francisco, CA.
29. Pettigrew, G. W., Aviram, I., and Schejter, A. (1976) The role of the lysines in the alkaline heme-linked ionization of ferric cytochrome *c*, *Biochem. Biophys. Res. Commun. 68*, 807−813.
30. Peterson, G. L. (1983) in *Enzyme Structure, Part I* (Hirs, C. H. W., and Timasheff, S. N., Eds.) pp 95−119, Academic Press, New York.
31. Bradford, M. M. (1976) A rapid and sensitive method for the quantitation of microgram quantities of protein utilizing the principle of protein−Dye binding, *Anal. Biochem. 72*, 248−254.
32. Compton, S. J., and Jones, C. G. (1985) Mechanism of dye response and interference in the Bradford protein assay, *Anal. Biochem. 151*, 369−374.
33. Thompson, G. S., Leung, Y. C., Ferguson, S. J., Radford, S. E., and Redfield, C. (2000) The structure and dynamics in solution of Cu(I) pseudoazurin from *Paracoccus pantotrophus*, *Protein Sci. 9*, 846−858.
34. Jones, S., Reader, J. S., Healy, M., Capaldi, A. P., Ashcroft, A. E., Kalverda, A. P., Smith, A. D., and Radford, S. E. (2000) Partially unfolded species populated during equilibrium denaturation of the β-sheet protein Y74W Apo-pseudoazurin, *Biochemistry 39*, 5672−5682.
35. Morelli, X., Czjzek, M., Hatchikian, C. E., Bornet, O., Fontecilla-Camps, J. C., Palma, N. P., Moura, J. J. G., and Guerlesquin, F. (2000) Structural model of the Fe-hydrigenase/cytochrome c_{553} complex combining transverse relaxation-optimized spectroscopy experiments and soft docking calculations, *J. Biol. Chem. 275*, 23204−23210.
36. Goodhew, C. F., Pettigrew, G. W., Devreese, B., Van Beeumen, J., Van Spanning, R. J. M., Baker, S. C., Saunders, N., Ferguson, S. J., and Thompson, I. P. (1996) The cytochrome c_{550} of *Paracoccus denitrificans* and *Thiosphaera pantotropha*: A need for re-evaluation of the history of *Paracoccus* cultures, *FEMS Microbiol. Lett. 137*, 95−101.
37. Van Spanning, R. J. M., de Boer, A. P. N., Reijnders, W. N. M., Westerhoff, H. V., Stouthamer, A. H., and van der Oost, J. (1997) FnrP and NNR of *Paracoccus denitrificans* are both members of the FNR family of transcriptional activators but have distinct roles in respiratory adaptation in response to oxygen limitation, *Mol. Microbiol. 23*, 893−907.
38. Otten, M. F., Stork, D. M., Reijnders, W. N., Westerhoff, H. V., and Van Spanning, R. J. (2001) Regulation of expression of terminal oxidases in *Paracoccus denitrificans*, *Eur. J. Biochem. 268*, 2486−2497.
39. Kakutani, T., Watanabe, H., K., A., and Beppu, T. (1981) A blue protein as an inactivating factor for nitrite reductase from *Alcaligenes faecalis* S-6, *J. Biochem. 89*, 463−472.
40. Suzuki, S., Sakurai, T., Shidara, S., and Iwasaki, H. (1989) Spectroscopic characterization of cobalt(II)-substituted *Achromobacter* pseudoazurin: Similarity of the metal center in Co(II)-pseudoazurin to those in Co(II)-plastocyanin and Co(II)-plantocyanin, *Inorg. Chem. 28*, 802−804.
41. Wehrfritz, J., Reilly, A., Spiro, S., and Richardson, D. J. (1993) Purification of hydroxylamine oxidase from *Thiosphaera pantotropha*—Identification of electron acceptors that couple heterotrophic nitrification to aerobic denitrification, *FEBS Lett. 335*, 246−250.
42. Kukimoto, M., Nishiyama, M., Ohnuki, T., Turley, S., Adman, E. T., Horinouchi, S., and Beppu, T. (1995) Identification of interaction site of pseudoazurin with its redox partner, copper-containing nitrite reductase from *Alcaligenes faecalis* S-6, *Protein Eng. 8*, 153−158.

43. Castro, G., Boswell, C. A., and Northrup, S. H. (1998) Dynamics of protein−protein docking: Cytochrome *c* and cytochrome *c* peroxidase revisited, *J. Biomol. Struct. Dyn. 16*, 413−424.
44. Murphy, L. M., Dodd, F. E., Yousafzai, F. K., Eady, R. R., and Hasnain, S. S. (2002) Electron donation between copper containing nitrite reductases and cupredoxins: The nature of protein−protein interaction in complex formation, *J. Mol. Biol. 315*, 859−871.
45. Krebs, J. J., Hauser, H., and Carafoli, E. (1979) Asymmetric distribution of phospholipids in the inner membrane of beef heart mitochondria, *J. Biol. Chem. 254*, 5308−5316.
46. Wilkinson, B. J., Morman, M. R., and White, D. C. (1972) Phospholipid composition and metabolism of *Micrococcus denitrificans*, *J. Bacteriol. 112*, 1288−1294.
47. Vakoufari, E., Wilson, K. S., and Petratos, K. (1994) The crystal structures of reduced pseudoazurin from *Alcaligenes faecalis* S-6 at two pH values, *FEBS Lett. 347*, 203−206.
48. Petratos, K., Banner, D. W., Beppu, T., Wilson, K. S., and Tsernoglou, D. (1987) The crystal structure of pseudoazurin from *Alcaligenes faecalis* S-6 determined at 2.9 Å resolution, *FEBS Lett. 218*, 209−214.
49. Inoue, T., Nishio, N., Suzuki, S., and Kataoka, K. (1999) Crystal structure determinations of oxidized and reduced pseudoazurins from *Achromobacter cycloclastes*, *J. Biol. Chem. 274*, 17845−17852.

BI0491144